Metal-phosphorus network on Pt(111)

Junqiu Zhang[1§], Xingxing Dong [2§], Shaogang Xu[2], Yipu Xia[1], Wingkin Ho[1], Hu Xu[2*], Maohai Xie[1*]

[1]*Department of Physics, The University of Hong Kong, Pokfulam Road, Hong Kong, 999077, China*

[2]*Department of Physics, Southern University of Science and Technology, Shenzhen, Guangdong 518055, China*

§ These authors contributed equally to this work.

*Authors to whom any correspondence should be addressed:

Email: xuh@sustech.edu.cn and mhxie@hku.hk.

Keywords: phosphorus; metal-phosphorus network; epitaxy; STM; DFT.

Abstract

Phosphorus (P) has been predicted to possess many two-dimensional (2D) allotropes, which have attracted intensive research attention due to their excellent properties and application promises. While only 2D black P films have been successfully obtained by the exfoliation method, fabrication of other phosphorus structures by epitaxial growth remains challenging. Recently, the metal-phosphorus network (MPhoN), a superstructure consisted of P and metal atoms has been realized, which offers a wider platform to study P and related compounds. In this paper, we report the observation of platinum-phosphorus networks (PtPhoNs) obtained by P adsorption on Pt(111). Our findings not only enrich the diverse structures of the MPhoN family but also provide insights into the formation mechanism of epitaxial P and its interaction with the noble metal substrate.

Introduction

Since the successful isolation of graphene, various layered two-dimensional (2D) crystalline films have been obtained and under extensive research attentions. These include transition-metal dichalcogenides[1-4], GaSe[5, 6], silicene[7, 8], tellurene[9, 10] and phosphorene[11-14]. The latter, i.e., black phosphorus monolayer, has drawn particular attention due to its superior semiconducting properties for low-dimensional optoelectronic devices[13-17]. Phosphorous (P) has five valence electrons and affords diverse bonding configurations between P atoms[18]. Besides black-P, various 2D phosphorus allotropes[18-21] make the system rich in properties and attractive for scientific research. In order to obtain high-quality samples of the other 2D phosphorus allotropes, molecular-beam epitaxy (MBE) growth on metal single crystals has been studied extensively[22-27]. Due to the diversity of P-metal interaction, the structural features of the deposits are dependent on the given metal substrates as well as the experimental conditions. For example, phosphorus clusters dispersed on Cu(111)[23], phosphorus nanobase arrays on Cu(110)[28], phosphorus pentamers[24], clusters[25] and quasi-one-dimensional phosphorus chains[27] on Ag(111) under different experimental conditions, and the gold-phosphorus network (AuPhoN) on Au(111) surfaces[22, 26] have been observed. In particular, precious metal phosphide constitutes a new catalyst platform owing to its multifunctional active site and novel chemical properties[29-31]. Recent studies have shown that the AuPhoN can be applied to selectively trap atoms or molecules, such as Sn[32], water[33], etc. Moreover, AuPhoN could be used as a substrate to grow monolayer and multilayer perylenetetracarboxylic dianhydride (PTCDA) films[34]. Thus, experimentally realizing more metal-phosphorus networks (MPhoNs) becomes increasingly attractive and important.

Platinum (Pt) is a catalytic material with excellent physical and chemical properties and is a common substrate for epitaxial growth of two-dimensional materials[35-38]. In this paper, we report the observation of platinum-phosphorus network (PtPhoN) superstructures grown by MBE of P on Pt(111). By combining experiments and density functional theory (DFT) calculations, we have deciphered the

atomic structure and electronic characteristics of the PtPhoNs, enriching the family of MPhoN surface superstructures. The findings provide valuable references for further studies of MPhoN epitaxial growth and P-metal interaction.

Method

Phosphorus deposition and subsequent low-temperature scanning tunneling microscopy and spectroscopy (LT-STM/S) measurements were conducted in a Unisoku UHV system having the base pressure of $<1 \times 10^{-10}$ Torr. Single-crystal Pt(111) substrate was cleaned by successive Ar ion bombardment (1.5 kV, 5×10^{-6} Torr) and annealing at ~700°C. It was held at temperatures in the range of 200~700°C for P film deposition. Phosphorus flux was generated by decomposing InP in a standard Knudsen cell at ~460°C and was estimated to be $\sim 2.1 \times 10^{11}$ molecules/cm^2·s. Decomposing InP compound led to relatively low but more controllable P fluxes than that using elemental P and yet it afforded relatively low operating temperature than other compounds such as GaP. Under the UHV condition of MBE, decomposing InP led to P vapor and indium liquid. Indium vapor, if any, was further block from reaching the sample by a mechanical shutter or 'diaphragm' put in front of the crucible, ensuring high purity of the deposit. After a coverage of phosphorus was deposited, the sample was quenched transferred immediately to the STM stage held at 77 K for surface characterizations. Constant-current mode of STM measurements was adopted, and the tunneling current was set at 100 pA.

First-principles calculations were performed by using the Vienna *ab initio* simulation package (VASP)[39, 40], based on density functional theory (DFT)[41, 42]. The projector augmented wave (PAW) method was employed to treat the core-valence interactions[43-45]. The generalized gradient approximation (GGA) with the Perdew-Burke-Ernzerhof (PBE) formalism was used for structural optimization and total energy calculations[46]. The force convergence criteria and kinetic-energy cutoff were set at 0.02 eV/Å and 400 eV respectively. A slab model with 5 layers of metal atoms was adopted for the study, and the vacuum layer thickness was set to 15 Å to avoid interaction between two neighboring images. In the process of geometric

optimization, the bottom two layers of the metal are fixed to simulate the bulk structure.

To describe the stability of P-containing structures on Pt(111) substrate, the formation energy (E_f) defined as[26, 47, 48]:

$$E_f = \left(E_{total} - E_{sub} - n_{Pt} \times \mu_{Pt} - n_p \times \mu_p\right)/n_p$$

were compared, where E_{total} is the total energy of the system, and E_{sub} is that of the substrate; μ_{Pt} and μ_p are chemical potentials of Pt and P, which represent the energies per Pt or P atom in the bulk phase, respectively; n_{Pt} and n_p are the numbers of Pt atoms (if any) and P atoms in the epilayer. The other calculation details are presented in the supplementary material.

Results and Discussion

Depositing a low coverage of P leads to the adsorption of P atoms on the Pt(111) surface. **Figure 1(a)** captures a state in a STM micrograph of the surface that has become fully covered by P adatoms. In the micrograph, each bright spot represents a P atom and the nearest neighbor distance is ~0.56 nm, i.e., twice the lattice constant of Pt(111). Low-energy electron diffraction (LEED) pattern shown in **Figure 1(b)** reveals consistently a (2×2)-reconstructed surface, thus it has a P coverage of ~0.25 monolayers (MLs). Here 1 ML is defined as one P adatom per Pt(111) surface site.

DFT calculations are performed to compare the adsorption energies of P on Pt(111) at three possible adsorption sites, i.e., the fcc, hcp, and the top sites (see **Figures 1(c)**). The calculated results are -2.309 eV (fcc), -2.250 eV (hcp) and -0.234 eV (top), respectively, showing that the fcc site is the most favorable adsorption site for P-on-Pt(111). Compared with the adsorption energy of P atom on Au(111) (-0.203 eV), the adsorption interaction of P atom on Pt(111) is much stronger. The enhancement of adsorbate-substrate interaction for P-on-Pt is presumably related to the partially filled d-orbitals of Pt whereas they are completely filled for Au[49]. Besides, our calculations of Bader charge, taking one P adatom on a 3×3 metal supercell as an example, show 0.45e transfer from P to Pt on Pt(111), whereas it is

only 0.26*e* from P to Au on Au(111). Since the 2D Au-P network has previously been reported, the stronger Pt-P interaction would imply strong tendency of forming Pt-P alloy with continuous depositions. Indeed, various superstructures have been observed in subsequent growth, which will be introduced later.

To further understand the behavior of P atoms on Pt(111) surface, the interactions between Pt and P atoms on Pt(111) have been investigated in more detail (see supplementary material **Figure S1)**. We note based on the strengths of possible interactions that P atoms on Pt(111) surface tend to repel each other. Therefore, we suggest that in the most stable P-Pt system, there should be no P-P bond in the alloy. This general principle will guide our investigations of the following P-Pt structures.

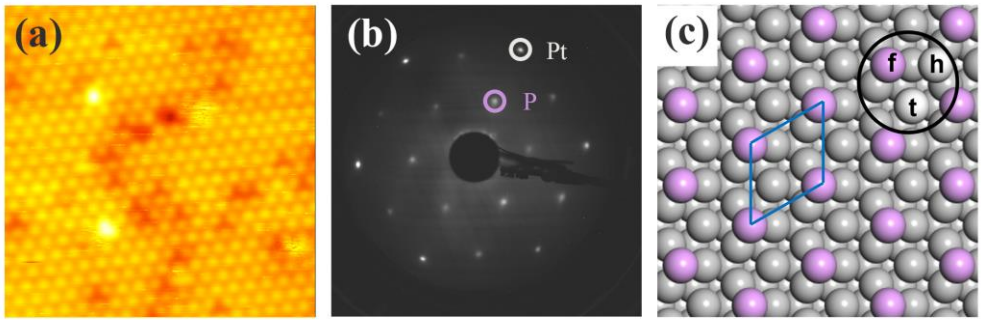

Figure 1. The (2×2)-reconstructed surface on Pt(111). (a) STM image (size: 10 × 10 nm^2; V_{sample} = -0.4 V) showing a (2×2)-reconstructed surface. (b) A LEED pattern of the (2×2)-reconstructed surface, where the 1×1 spots of Pt and P are marked by white and purple circles respectively. The incident electron energy is 70 eV. (c) A model of the (2×2)-reconstructed surface. The circle highlights P atoms (purple and white) adsorbed on the fcc (marked with f), hcp (marked with h), and top (marked with t) site of Pt(111) (gray) surface respectively.

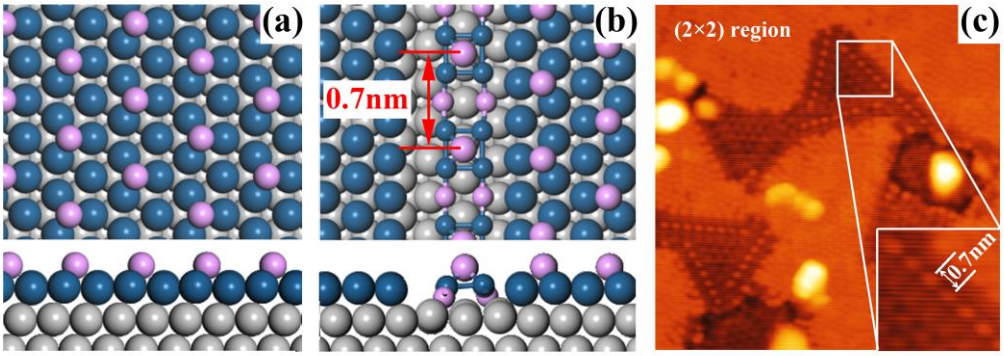

Figure 2. Schematic diagram showing the formation of the Pt_4P nanoblocks. (a) The (2×2)-reconstructed surface. The pink and blue spheres are P and the surface Pt atoms, where the gray spheres represent the Pt substrate. (b) The Pt_4P nanoblocks connected by P atoms on Pt(111). (c) STM image (size: 23 × 23 nm^2; V_{sample} = 1 V) of a sample revealing bright lines near the edges of triangular voids, where the distance between neighboring bright spots on the lines is about 0.7 nm (inset).

Further deposition of P atoms upon a surface that is almost completely covered by adsorbed P atoms (**Figure 1**) at ~400℃ for ~10 min results in a new structure showing triangular voids embroidered by bright lines in STM as exemplified in **Figure 2(c)**. Large-scale and close-up STM images are presented in **Figure S2**. Such a new structure forms likely due to the increased surface coverage of P by the continuous deposition, or due to the prolonged 'annealing' of the sample at the elevated temperature while maintaining surface P coverage. Close examinations of the STM images reveal an ordered distorted-hexagon-ring structure in the triangular void, which shows an apparent height that is lower than the surrounding (2×2)-adsorption region by exactly that of the P adatom layer. The precise nature of this void region remains unknown. On the other hand, the appearance of the embroidered bright lines in the voids but close to the boundary with the (2×2)-adsorption region may evidence alloying between P and Pt.

Figure 2(a) and **(b)** depict our conjectured atomic structures before and after the alloying respectively, by adsorbing P atoms. Before alloying, P coverage of the (2×2)-reconstructed surface was 0.25 ML (**Figure 2(a)**). By further depositing P

and/or annealing, the P atoms will react and alloy with Pt in substrate, forming interconnected Pt_4P nanoblocks. Each Pt_4P nanobloack consists of four Pt atoms arranged in a square at the bottom and one P atom bonded to these Pt atoms at the top (**Figure 2(b)**). We note that the measured distance between the bright spots on the bright lines in the STM image is about 0.7 nm (see **Figure 2(c)** inset), which corresponds exactly to the distance calculated between adjacent nanoblocks.

We use the Pt_4P nanoblock structure as the basis for various splices and combinations by the RG^2 code[50] **(Figure S3)** and find that the formation energies for many structures are close, which can be explained by the similar local motifs in these 2D allotropes. Among them, PtPhoN (see **Figures 3** and **S3(f)**) and platinum phosphorus chains (PtPhoC) (see **Figures 4** and **S3(h)**) are experimentally observed. These two superstructures can be obtained by continuous adsorption of P atoms (e.g., for ~ 10 min) on the surface of **Figure 2(c)** at temperatures between 200 and 700℃. The coverage of these two superstructures becomes more dominant as the surface temperature is higher. Indeed, at about 500~700℃, the sample surface can be fully covered by PtPhoN/C, given enough deposition time. On the other hand, these latter two superstructures were found to almost always co-exist, occupying different terraces on the same substrate surface (see **Figure 4(a)**), suggesting the formation energy degeneracy of the two structures (see below).

Figure 3(a) presents an STM image revealing the PtPhoN superstructure that is most commonly seen. The morphology of this structure consists of hexagonal rings with three bright spots at each corner, three additional but faint and irregularly orientated spots inside the hexagonal ring. The distance between the centers of adjacent rings is ~1.8 nm. This structure is believed to be the same as the one reported previously by direct deposition of P on Pt(111)[51], where electron diffraction showed the $\left(4\sqrt{3}\times 4\sqrt{3}\right)R30^o$ pattern (**Figure 3(b)**). Heikkinen *et al.* proposed a model consisted of P_{13} or P_{14} clusters, where each P_{13}/P_{14} cluster presents a corner in the ring[51]. Our DFT calculations however point favorably to a different and more viable model. In essence, as elaborated earlier, due to the strong interaction between P

and Pt, P atoms preferably bond with Pt atoms forming a PtPhoN rather than being bonded with each other forming pure P clusters. As depicted in **Figure 3(c)**, the rings in our model are consisted of Pt_4P nanoblocks. Three Pt_4P nanoblocks form one corner of the hexagonal ring, and adjacent nanoblocks share the same Pt atom. Two adjacent corners in a hexagonal ring are connected by two P atoms located at the fcc and hcp sites respectively (**Figure S3(f)**). Simulated STM images of this model are seen to match well with the experimental observations (**Figure 3(c)**).

We have compared the formation energies of the different models proposed previously, including the P_{14}-cluster model (P_{13} model is unstable)[51], BlueP monolayer, and different compositions of the platinum phosphorus alloys: Pt_6P_8, Pt_9P_{18}, $Pt_{12}P_{32}$, and $Pt_{15}P_{50}$[52] **(Figure S4)**. The results are summarized in **Figure 3(d)**. Clearly, the PtPhoN model as proposed in **Figure 3(c)** is energetically more favorable than the others, which is also the most stable one among all the candidates we have examined.

As for the three additional spots inside the hexagonal ring observed in the experiment, the previous study suggested that each of such spots represented an unbonded P_4 cluster trapped inside the ring[51]. We believe this is unlikely the case, and P_4 clusters would be inconsistent with the P-P repulsive nature of bonding on the Pt(111) surface. These three faint bright spots could be alloy clusters or adsorbed P atoms. If so, it would imply that the abundant rings in this PtPhoN can be useful to trap other desired atoms or molecules, which invites further studies.

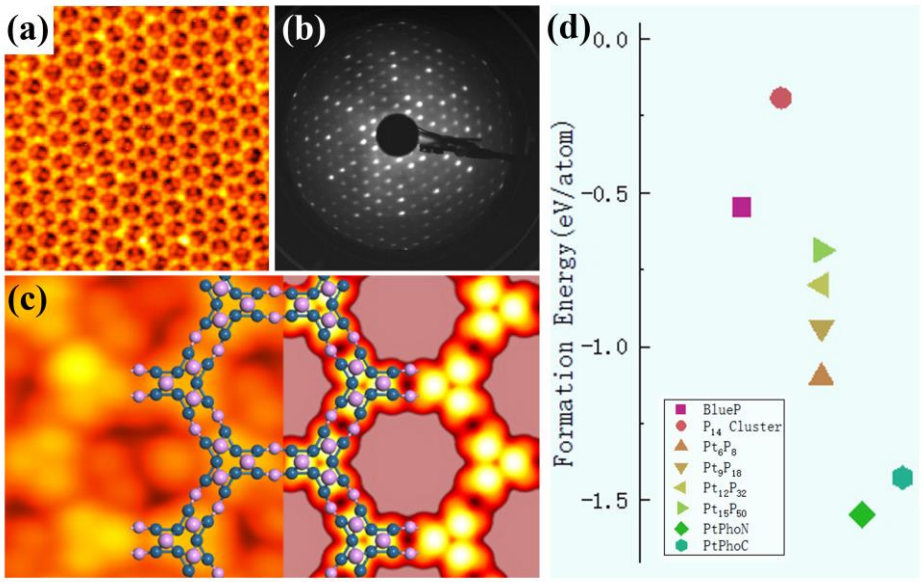

Figure 3. The PtPhoN structure. (a) STM image revealing the structural details of the $(4\sqrt{3} \times 4\sqrt{3})R30°$ surface (size: 20 × 20 nm^2; V_{sample} = 0.1 V). (b) LEED pattern of the $(4\sqrt{3} \times 4\sqrt{3})R30°$ surface (incident electron energy = 70 eV). (c) The calculated structure of the PtPhoN model overlaid on the experiment image (left) and the simulated STM image (right). (d) Comparison of formation energies of different structural models. The P_{14}-clusters model and platinum phosphorus alloys are respectively reported in Refs. [51] and [52].

Besides the PtPhoN structure described above, experimentally we discover a new ordered structure of the P-Pt surface (the left panel of **Figure 4(a)**) that has not been documented previously. It has a rectangular unit cell of size $a = 0.7$ nm, $b = 1.2$ nm, as labeled in **Figure 4(b)**. Interestingly, although the symmetry is very different, this structure appears to always co-exist with the PtPhoN. We propose that this new structure, called the PtPhoC, is that as shown in **Figure 4(b)** top panel, in which the Pt_4P nanoblocks are simply linked into long chains by P atoms. The simulated STM image of such a model again matches well with the experiment (see **Figure 4(b)** bottom panel). At the same time, we suspect that there may be adsorbed P atoms between the two chains at high concentrations. The formation energies of the PtPhoN and PtPhoC are comparable (see **Figure 3(c)**), which explains why we usually

observe these two structures at the same time in the experiment.

In addition to the PtPhoN and PtPhoC superstructures described above, there is also a square-lattice structure that we have observed during the deposition process, which corresponds to a higher P coverage. More details about this structure are introduced in **Figure S5**. It may also belong to the Pt-P alloys, though its atomic configuration remains to be identified.

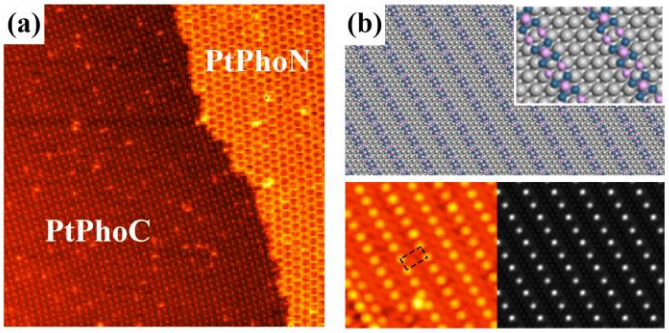

Figure 4. The PtPhoC structure. (a) STM image (size: 60 × 60 nm^2; V_{sample} = -1 V) showing the co-existence of the PtPhoC structure (left) and the PtPhoN structure (right), occupying different Pt terraces. (b) The proposed structural model of the PtPhoC (top), experiment image (bottom left), and the simulated STM image (bottom right). The pink and blue spheres are P and Pt atoms in the PtPhoC, where the gray spheres represent the Pt substrate.

Conclusion

In summary, we have synthesized two new structures of the precious metal phosphide by depositing P on the Pt(111) surface. Their morphologies and atomic structures are carefully investigated by STM and DFT calculations. Moreover, we investigated their formation mechanism, where strong interaction between P and Pt(111) makes the adsorbed P atoms to alloy with Pt, forming the square Pt_4P nanoblocks. These Pt_4P nanoblocks can be linked by P atoms to generate PtPhoN or PtPhoC by sharing the Pt atoms in the nanoblocks. These findings have not only enriched the MPhoN family but also provided new insights into the P-noble metal interaction.

Acknowledgement

We have benefitted from discussions and help from J.-P. Xu, H. Tian and Y. J. Jin. The project is financially supported by grants from the Research Grant Council of Hong Kong Special Administrative Region, China (Nos. 17304318 and AoE/P-701/20) and the National Natural Science Foundation of China (No. 11974160).

Data availability statement

The data that support the findings of this study are available upon reasonable request from the authors.

References

[1] Mak K F, Lee C, Hone J, Shan J and Heinz T F 2010 Atomically Thin MoS2: A New Direct-Gap Semiconductor *Physical Review Letters* **105** 136805

[2] Wang Q H, Kalantar-Zadeh K, Kis A, Coleman J N and Strano M S 2012 Electronics and optoelectronics of two-dimensional transition metal dichalcogenides *Nature Nanotechnology* **7** 699

[3] Liu H, Jiao L, Yang F, Cai Y, Wu X, Ho W, Gao C, Jia J, Wang N and Fan H 2014 Dense network of one-dimensional midgap metallic modes in monolayer MoSe2 and their spatial undulations *Physical Review Letters* **113** 066105

[4] Jiao L, Liu H J, Chen J, Yi Y, Chen W, Cai Y, Wang J, Dai X, Wang N and Ho W K 2015 Molecular-beam epitaxy of monolayer MoSe2: growth characteristics and domain boundary formation *New Journal of Physics* **17** 053023

[5] Hu P, Wen Z, Wang L, Tan P and Xiao K 2012 Synthesis of Few-Layer GaSe Nanosheets for High Performance Photodetectors *ACS Nano* **6** 5988-94

[6] Late D J, Liu B, Matte H S S R, Rao C N R and Dravid V P 2012 Rapid Characterization of Ultrathin Layers of Chalcogenides on SiO2/Si Substrates *Advanced Functional Materials* **22** 1894-905

[7] Vogt P, De Padova P, Quaresima C, Avila J, Frantzeskakis E, Asensio M C, Resta A, Ealet B and Le Lay G 2012 Silicene: Compelling Experimental Evidence for Graphenelike Two-Dimensional Silicon *Physical Review Letters* **108** 155501

[8] Chen L, Liu C-C, Feng B, He X, Cheng P, Ding Z, Meng S, Yao Y and Wu K 2012 Evidence for Dirac Fermions in a Honeycomb Lattice Based on Silicon *Physical Review Letters* **109** 056804

[9] Huang X, Guan J, Lin Z, Liu B, Xing S, Wang W and Guo J 2017 Epitaxial

Growth and Band Structure of Te Film on Graphene *Nano Letters* **17** 4619-23
[10] Chen J, Dai Y, Ma Y, Dai X, Ho W and Xie M 2017 Ultrathin β-tellurium layers grown on highly oriented pyrolytic graphite by molecular-beam epitaxy *Nanoscale* **9** 15945-8
[11] Liu H, Neal A T, Zhu Z, Luo Z, Xu X, Tománek D and Ye P D 2014 Phosphorene: An Unexplored 2D Semiconductor with a High Hole Mobility *ACS Nano* **8** 4033-41
[12] Tran V, Soklaski R, Liang Y and Yang L 2014 Layer-controlled band gap and anisotropic excitons in few-layer black phosphorus *Physical Review B* **89** 235319
[13] Li L, Yu Y, Ye G J, Ge Q, Ou X, Wu H, Feng D, Chen X H and Zhang Y 2014 Black phosphorus field-effect transistors *Nature Nanotechnology* **9** 372
[14] Xia F, Wang H and Jia Y 2014 Rediscovering black phosphorus as an anisotropic layered material for optoelectronics and electronics *Nature Communications* **5** 4458
[15] Qiao J, Kong X, Hu Z-X, Yang F and Ji W 2014 High-mobility transport anisotropy and linear dichroism in few-layer black phosphorus *Nature Communications* **5** 4475
[16] Song H, Wu H, Ren T, Yan S, Chen T and Shi Y 2021 Developments in stability and passivation strategies for black phosphorus *Nano Research* **14** 4386-97
[17] Ling Z, Li P, Zhang S-Y, Arif N and Zeng Y-J 2022 Stability and passivation of 2D group VA elemental materials: black phosphorus and beyond *Journal of Physics: Condensed Matter* **34** 224004
[18] Guan J, Zhu Z and Tománek D 2014 Phase Coexistence and Metal-Insulator Transition in Few-Layer Phosphorene: A Computational Study *Physical Review Letters* **113** 046804
[19] Zhu Z and Tománek D 2014 Semiconducting Layered Blue Phosphorus: A Computational Study *Physical Review Letters* **112** 176802
[20] Kaur S, Kumar A, Srivastava S and Tankeshwar K 2016 Electronic structure engineering of various structural phases of phosphorene *Physical Chemistry Chemical Physics* **18** 18312-22
[21] Zeng J, Cui P and Zhang Z 2017 Half Layer By Half Layer Growth of a Blue Phosphorene Monolayer on a GaN(001) Substrate *Physical Review Letters* **118** 046101
[22] Xu J-P, Zhang J-Q, Tian H, Xu H, Ho W and Xie M 2017 One-dimensional phosphorus chain and two-dimensional blue phosphorene grown on Au(111) by molecular-beam epitaxy *Physical Review Materials* **1** 061002
[23] Zhou D, Meng Q, Si N, Zhou X, Zhai S, Tang Q, Ji Q, Zhou M, Niu T and Fuchs H 2020 Epitaxial Growth of Flat, Metallic Monolayer Phosphorene on Metal Oxide *ACS Nano* **14** 2385-94
[24] Zhang W, Enriquez H, Tong Y, Mayne A J, Bendounan A, Dappe Y J, Kara A, Dujardin G and Oughaddou H 2020 Phosphorus Pentamers: Floating Nanoflowers form a 2D Network *Advanced Functional Materials* **30** 2004531

[25] Yang S, Hu Z, Wang W, Cheng P, Chen L and Wu K 2020 Regular Arrangement of Two-Dimensional Clusters of Blue Phosphorene on Ag(111) *Chin. Phys. Lett.* **37** 096803
[26] Tian H, Zhang J-Q, Ho W, Xu J-P, Xia B, Xia Y, Fan J, Xu H, Xie M and Tong S Y 2020 Two-Dimensional Metal-Phosphorus Network *Matter* **2** 111-8
[27] Zhang W, Enriquez H, Tong Y, Mayne A J, Bendounan A, Smogunov A, Dappe Y J, Kara A, Dujardin G and Oughaddou H 2021 Flat epitaxial quasi-1D phosphorene chains *Nature Communications* **12** 5160
[28] Zhang J L, Zhao S, Sun S, Niu T, Zhou X, Gu C D, Han C, Yuan K D, Guo R, Wang L, Li Z and Chen W 2017 Phosphorus Nanostripe Arrays on Cu(110): A Case Study to Understand the Substrate Effect on the Phosphorus thin Film Growth *Advanced Materials Interfaces* **4** 1601167
[29] Bowker R H, Smith M C, Pease M L, Slenkamp K M, Kovarik L and Bussell M E 2011 Synthesis and Hydrodeoxygenation Properties of Ruthenium Phosphide Catalysts *ACS Catalysis* **1** 917-22
[30] Kanda Y, Kawanishi K, Tsujino T, Al-otaibi A M and Uemichi Y 2018 Catalytic Activities of Noble Metal Phosphides for Hydrogenation and Hydrodesulfurization Reactions *Catalysts* **8** 160
[31] Pu Z, Liu T, Zhao W, Shi X, Liu Y, Zhang G, Hu W, Sun S and Liao S 2020 Versatile Route To Fabricate Precious-Metal Phosphide Electrocatalyst for Acid-Stable Hydrogen Oxidation and Evolution Reactions *ACS Applied Materials & Interfaces* **12** 11737-44
[32] Zhang J L, Zhao S, Sun S, Wang W, Ma Z, Lian X, Li Z and Chen W 2021 Atom by Atom Condensation of Sn Single Clusters within Gold–Phosphorus Metal–Inorganic Porous Networks *The Journal of Physical Chemistry Letters* **12** 745-51
[33] Si N, Shen T, Zhou D, Tang Q, Jiang Y, Ji Q, Huang H, Liu W, Li S and Niu T 2019 Imaging and Dynamics of Water Hexamer Confined in Nanopores *ACS Nano* **13** 10622-30
[34] Gruenewald M, Schaal M, Karadzhov I, Brill L, Domke J, Grimm P, Otto F, Picker J, Simon P M, Tamm H, Fritz T and Forker R 2022 Blue phosphorene on Au(111) as a decoupling layer for organic epitaxially grown films *Physical Review Materials* **6** 015601
[35] Maurice V, Salmeron M B and Somorjai G A 1990 The epitaxial growth of zirconium oxide thin films on Pt(111) single crystal surfaces *Surface Science* **237** 116-26
[36] Müller F, Stöwe K and Sachdev H 2005 Symmetry versus Commensurability: Epitaxial Growth of Hexagonal Boron Nitride on Pt(111) From B-Trichloroborazine (ClBNH)3 *Chemistry of Materials* **17** 3464-7
[37] Gao M, Pan Y, Huang L, Hu H, Zhang L Z, Guo H M, Du S X and Gao H-J 2011 Epitaxial growth and structural property of graphene on Pt(111) *Applied Physics Letters* **98** 033101
[38] Guo H, Jiménez-Sánchez M D, Martínez-Galera A J and Gómez-Rodríguez J M Unraveling the Highly Complex Nature of Antimony on Pt(111) *Advanced*

Materials Interfaces **9** 2101272

[39] Kresse G and Furthmüller J 1996 Efficient iterative schemes for ab initio total-energy calculations using a plane-wave basis set *Physical Review B* **54** 11169-86

[40] Kresse G and Furthmüller J 1996 Efficiency of ab-initio total energy calculations for metals and semiconductors using a plane-wave basis set *Computational Materials Science* **6** 15-50

[41] Hohenberg P and Kohn W 1964 Inhomogeneous Electron Gas *Physical Review* **136** B864-B71

[42] Kohn W and Sham L J 1965 Self-Consistent Equations Including Exchange and Correlation Effects *Physical Review* **140** A1133-A8

[43] Ceperley D M and Alder B J 1980 Ground State of the Electron Gas by a Stochastic Method *Physical Review Letters* **45** 566-9

[44] Blöchl P E 1994 Projector augmented-wave method *Physical Review B* **50** 17953-79

[45] Kresse G and Joubert D 1999 From ultrasoft pseudopotentials to the projector augmented-wave method *Physical Review B* **59** 1758-75

[46] Perdew J P, Burke K and Ernzerhof M 1996 Generalized Gradient Approximation Made Simple *Physical Review Letters* **77** 3865-8

[47] Dávila M E, Xian L, Cahangirov S, Rubio A and Le Lay G 2014 Germanene: a novel two-dimensional germanium allotrope akin to graphene and silicene *New Journal of Physics* **16** 095002

[48] Yin Y, Gladkikh V, Li P, Zhang L, Yuan Q and Ding F 2021 Stabilities of Isomers of Phosphorus on Transition Metal Substrates *Chemistry of Materials* **33** 9447-53

[49] Hammer B and Norskov J K 1995 Why gold is the noblest of all the metals *Nature* **376** 238-40

[50] Shi X, He C, Pickard C J, Tang C and Zhong J 2018 Stochastic generation of complex crystal structures combining group and graph theory with application to carbon *Physical Review B* **97** 014104

[51] Heikkinen O, Pinto H, Sinha G, Hämäläinen S K, Sainio J, Öberg S, Briddon P R, Foster A S and Lahtinen J 2015 Characterization of a Hexagonal Phosphorus Adlayer on Platinum (111) *The Journal of Physical Chemistry C* **119** 12291-7

[52] Zhao S and Li Z 2021 Blue Phosphorus Growth on Different Noble Metal Surfaces: From a 2D Alloy Network to an Extended Monolayer *The Journal of Physical Chemistry C* **125** 675-9